Structural and kinetic considerations for the application of the traceless Staudinger ligation to future 18F radiolabeling using XRD and 19F-NMR

Köckerling, M.; Mamat, C.;

Originally published:

November 2017

International Journal of Chemical Kinetics 50(2018), 31-40

DOI: https://doi.org/10.1002/kin.21137

X-ray studies on phosphanes and kinetic considerations of the traceless Staudinger Ligation for radiolabeling with fluorine-18 using ^{19}F-NMR

Martin Köckerling,[a] Constantin Mamat[b,*]

[a] Institut für Radiopharmazeutische Krebsforschung, Helmholtz-Zentrum Dresden-Rossendorf, Bautzner Landstraße 400, D-01328 Dresden, Germany

[b] Institut für Chemie, Anorganische Festkörperchemie, Universität Rostock, Albert-Einstein-Straße 3a, D-18059 Rostock, Germany

Tel: +49(351)2602915, e-mail: c.mamat@hzdr.de

Abstract

4-Fluorobenzoate-functionalized phosphane was reacted with benzyl azide using the traceless Staudinger Ligation to produce a fluorinated amide as a representative reaction for corresponding ^{18}F-radiolabeling reactions. The reaction kinetics was evaluated at different temperatures and the effect of starting material concentrations was investigated. ^{19}F-NMR was used to determine the reaction half-live ($\tau_{1/2}$) and the reaction rate constant (k_{obs}) of this reaction under mild reaction conditions in aqueous medium which are required for labeling of biomacromalecules. Furthermore, the phosphanol starting material **1** (orthorhombic, space group $Pna2_1$, a = 18.6363(9), b = 8.3589(4), c = 18.5480(9) Å, V = 2889.4(2) Å^3, Z = 8, D_{obs} = 1.277 g/cm^3) and the fluorine-containing phosphane **3** (monoclinic, space group $P2_1/c$, a = 8.321(2), b = 16.160(4), c = 14.940(4) Å, β = 99.51(1)°, V = 1981.4(8) Å^3, Z = 4, D_{obs} = 1.342 g/cm^3) were analyzed by single-crystal XRD.

Key words

Click – bioorthogonal – building blocks – kinetics – X-ray structure

1 Introduction

Both variants of Staudinger Ligation [1] belong to the most important biorthogonal conjugation reactions for site-selective labeling purposes [2,3] and proceed without any catalyst in contrast to other reactions (e.g. the Huisgen-click reaction) [4]. The absence of a metal catalyst (e.g. Cu) is important especially for *in vitro* and *in vivo* applications. Therefore, the traceless variant of the Staudinger Ligation [5,6,7] independently developed by Raines [8] and Bertozzi [9] is utilized for the connection of proteins [10,11], peptides and peptide fragments [8,12], the glycosylation [13] of amino acids and peptides [14,15], the preparation of large-sized lactams [16,17], the functionalization of polymers [18] and the introduction of radiolabels [19,20,21,22] and fluorescence dyes [23,24,25]. Both, the chemical modification of the biological active molecule and the preparation of the labeling building block are also quite facile. In general, one of the reactants is modified with azide [26,27] and the other is functionalized with a phosphane moiety [28,29]. This enables a fast reaction rate under mild reaction conditions (e.g. low reaction temperature, aqueous reaction medium), which is favorable especially for the introduction of radiolabels into sensitive bio(marco)molecules like proteins or antibodies [30,31], since the applied radionuclides often suffer from short half-live (e.g. ^{11}C: 20 min, ^{18}F: 109,8 min, ^{99m}Tc: 6 h) [32].

In the past, NMR was used to study the mechanism and the reaction rate of the Staudinger Ligation [33,34], but ^{13}C-labeled starting materials were used in the past to quantitatively determine the

spectra in a reasonable time span. To avoid performing circumstantial syntheses to prepare the ^{13}C-enriched starting materials, we focused on the application of ^{19}F NMR, since ^{19}F-containing derivatives were already available as reference compounds for the identification of the corresponding ^{18}F-radiotracers [35]. Thus, the ^{19}F nucleus is present in the starting material and the ligation product. In our case, the fluorine-containing phosphane **3** acts as starting material and gives amide **5** as the ligation product.

Fluorine-19 has favorable properties for NMR measurements like a nuclear spin of 1/2, a high magnetogyric ratio (0.94 x of ^{1}H) and it is 100% naturally enriched as ^{19}F (monoisotopic), [36] which makes this isotope highly responsive for fast and quantitative NMR measurements in the same manner as ^{1}H or ^{31}P. No further supplementary introduction or enrichment of NMR sensitive nuclides into one or both of the reactants is mandatory in contrast to $^{12}C/^{13}C$-measurements. In the past, ^{19}F-NMR has been used as an excellent tool for kinetic studies on chemical reactions [37,38].

Fast reactions are mandatory for labeling with the β^{+}-emitter fluorine-18 due to its short half-life of approx. 110 min [30,32,35]. Our objective was the development of a convenient method to determine the kinetics of the traceless Staudinger Ligation via ^{19}F-NMR. These results indicate the reaction rate using this ligation is for a future application in mild ^{18}F-labeling.

2 Results and Discussion

2.1 Synthesis and X-ray determination

Kinetic studies were performed to ensure the reaction rate is suitable for applying the traceless Staudinger ligation to future ^{18}F-radiolabeling. In general, functionalized phosphanes act as starting material for the Staudinger Ligation [5,6,7], while phosphanes with an electrophilic center (e.g. ester, thioester, amide) in close proximity to the phosphorus are required for the traceless variant. For this purpose, phosphane **3** serves as key compound [28] and was prepared by the reaction of phosphanol **1** with 4-fluorobenzoyl chloride (**2**) under basic conditions [39,40]. Next, phosphane **3** was reacted with benzyl azide (**4**) to give the desired Staudinger product **5** [41] and phosphane oxide **6**. Both reactions are shown in Scheme 1.

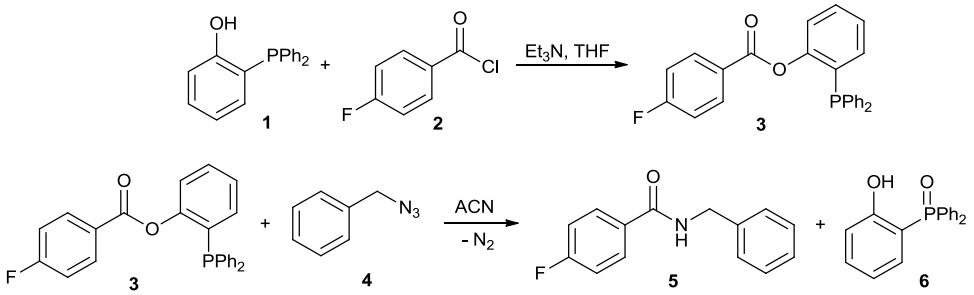

Scheme 1. Reaction of **1** and **2** to phosphane **3** and traceless Staudinger Ligation with of **3** with azide **4** to amide **5**.

Single crystals of phosphanol **1** and fluorine-containing phosphane **3** were obtained during the purification process and were characterized by single crystal X-ray analysis [42,43,[44]]. The molecular structures of **1** and **3** are illustrated in Figures 1 and 2. Crystals of **1** are composed of two symmetry independent molecules. The OH group in the molecule around P2 is disordered on two sites, labeled

O2A and O2B. In both compounds the residues around the P-atoms are arranged in a trigonal-pyramidal fashion with average C–P–C angles slightly smaller than the ideal tetrahedral value, i.e. for **1**, P1: 102.5°, P2: 102.7° and for **3**, P1: 102.8°. Whereas in **1** classical hydrogen bonding is not observed, in **3** one O–H···O contact (O2B–H2B···O1) with a donor–acceptor distance of 3.16(2) Å and a bond angle of 162.9° is observed.

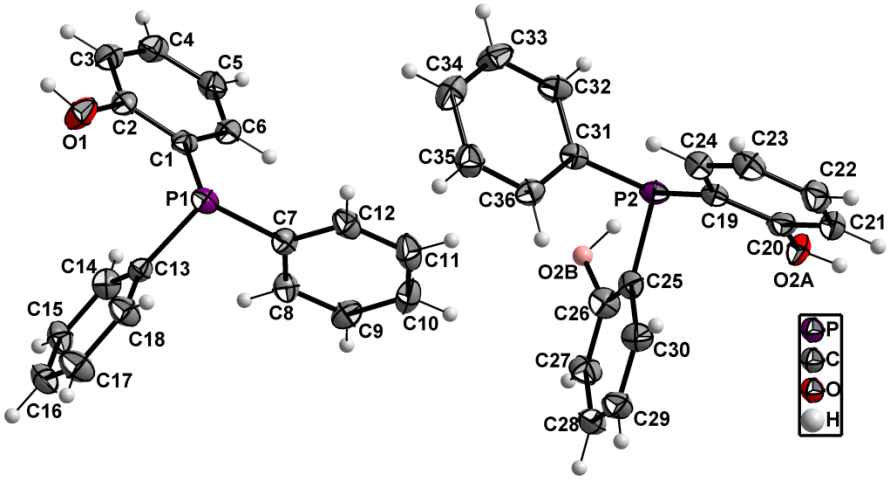

Figure 1: Structure of the two symmetry independent molecules of the phosphanol **1** (ORTEP plot, 50% probability level).

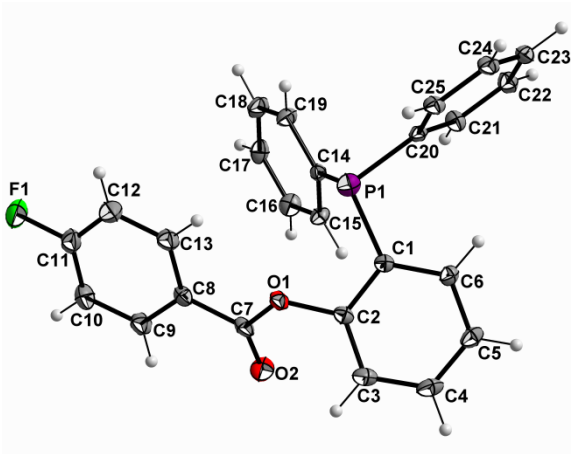

Figure 2: Molecular structure of fluorine-containing phosphane **3** (ORTEP plot, 50% probability level).

2.2 Determination of k_{obs} via ^{19}F-NMR

For analysis of the kinetic rates, it is necessary to distinguish between phosphane **3** and amide **5**, based on their different ^{19}F chemical shifts. The fluorine signal of starting material **3** was determined at δ = –106.1 ppm and the signal of the Staudinger product **5** at δ = –110.4 ppm in the ^{19}F NMR using a mixture of D_2O and acetonitrile-d_6 (ratio: *v*:*v* = 10:1). Additionally, the reaction was indirectly

monitored by ^{31}P NMR. The product **5** does not contain phosphorus, so the by-product **6** (δ = +35 ppm) was detected instead in addition to starting phosphane **3** (δ = –15 ppm).

Our study comprised of three experiments. The first two were based on the equimolar reaction of both starting materials **3** and **4** at temperatures of 25°C and 45°C, respectively. The low temperatures were chosen in consideration of future labeling reactions. Mild conditions are essential especially for labeling proteins or antibodies, which can be destroyed at elevated temperatures. For the third experiment, the reaction was performed with 10-fold excess of the starting azide **4** at 25°C to simulate conditions observed in radiolabeling procedures. Generally, the precursor (non-radioactive starting material) is always in high excess compared to the compound containing the radionuclide (radiolabeling building block) [30]. Due to the azide **4** (as prospective precursor) being 10-fold higher compared to the phosphane **3**, the pseudo first order conditions can be suposed [45].

All NMR-experiments were carried out in a mixture of acetonitrile-d_3 and D_2O (ratio: *v*:*v* = 10:1). A stock solution of phosphane **3** was prepared with a concentration of 71 nM. Solutions with azide **4** were prepared with final concentrations of 71 nM and 710 nM, respectively. At the beginning of the reaction, ^{19}F and ^{31}P NMR spectra were recorded at 3 to 15 minutes and, latter at 30 to 60 minutes. A representative record of ^{19}F and ^{31}P NMR spectra for the reaction of **3** with **4** in 10fold excess of **4** is displayed in Figures 3 and 4.

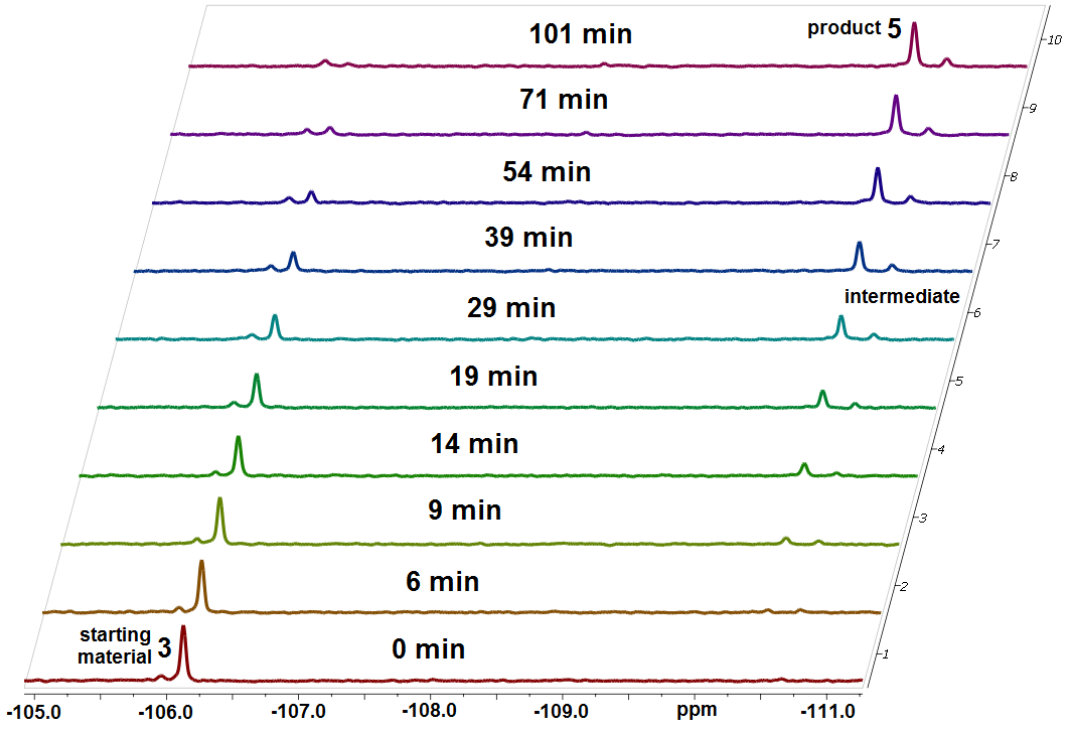

Figure 3. Representative set of ^{19}F-NMR spectra recorded on different time points to determine the reaction half-life $\tau_{1/2}$ and the rate constant for the reaction with 10fold excess of azide **4** at 25°C.

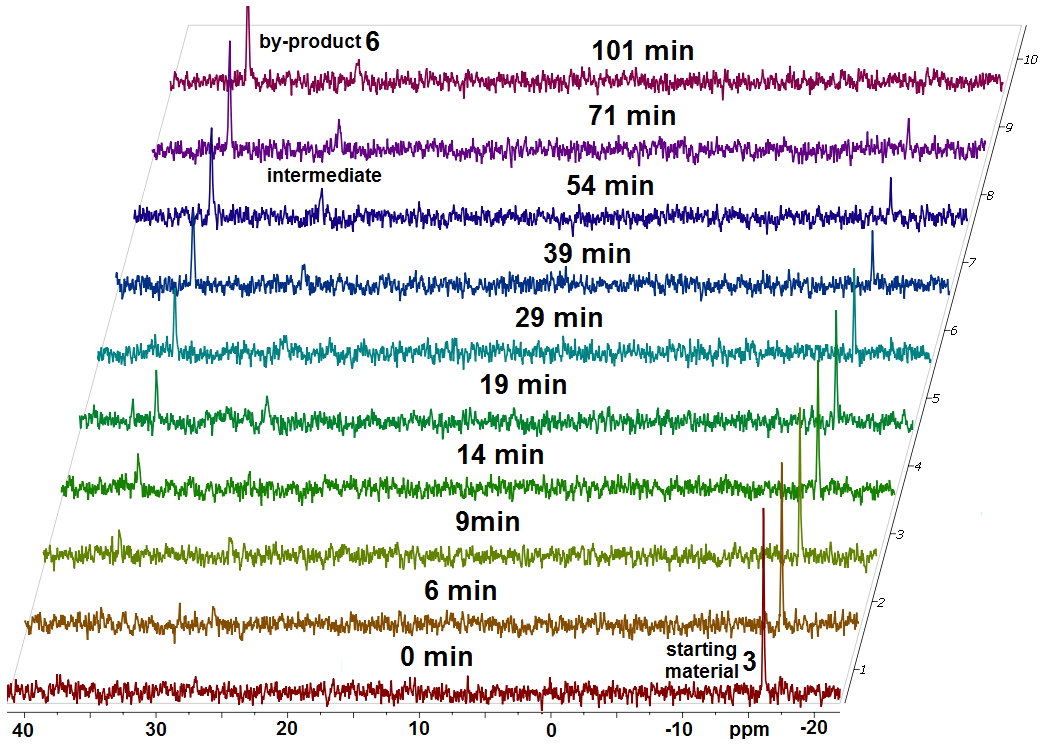

Figure 4. Representative set of ^{31}P-NMR spectra recorded on different time points to determine the reaction half-life $\tau_{1/2}$ and the rate constant for the reaction with 10fold excess of azide **4** at 25°C.

The reaction half-live $\tau_{1/2}$ was determined as good impression for the reaction rate of the traceless Staudinger Ligation. A summary of the data is found in Table 1. When comparing the dependence on the temperature, the reaction rate at 45°C is higher. Thus, $\tau_{1/2}$ = 52 min was found for the reaction at 45°C in contrast to $\tau_{1/2}$ = 211 min for the reaction at 25°C. The same result is found when comparing the reaction (1:1 ratio) with the reaction (10:1 ratio) at 25°C. For the reaction with 10-fold excess of azide **4**, the shortest reaction half-life of $\tau_{1/2}$ = 22 min was calculated. No starting material **3** was found after 92 min when using 10fold excess of azide **4** whereas starting material **3** from the equimolar reaction was still detected after 350 min. The results are visualized in Figure 5. Only slight differences between the results of the ^{19}F and the ^{31}P NMR measurements were observed.

Table 1: Summary of results from NMR measurements.

Molar ratio of starting materials	**Temperature**	**reaction half-live $\tau_{1/2}$**
phosphane **3** : azide **4** = 1:1	25°C	211 min
phosphane **3** : azide **4** = 1:1	45°C	52 min
phosphane **3** : azide **4** = 1:10	25°C	22 min

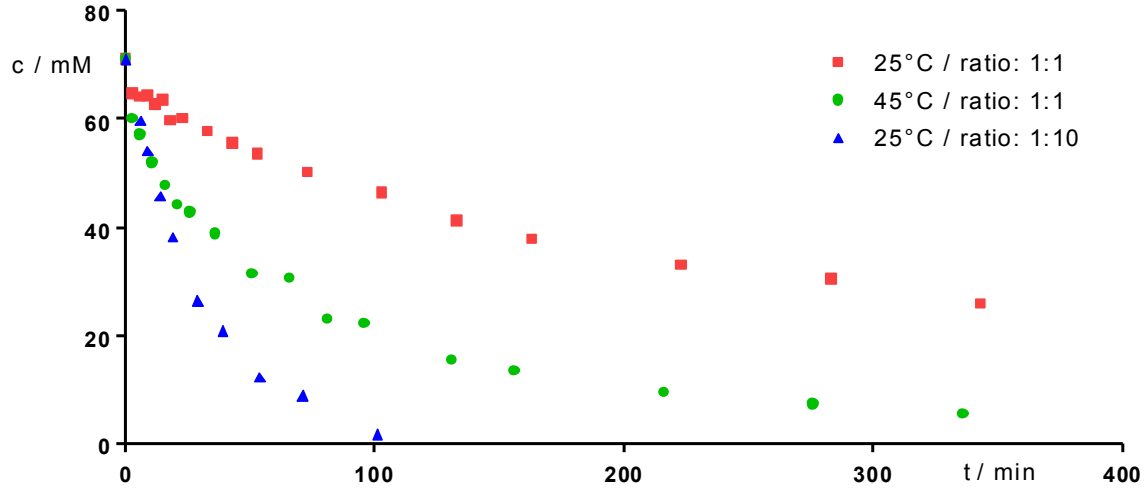

Figure 4: Decrease of concentration of phosphane **3** during Staudinger Ligations at different temperatures (25°C ■/▲; 45°C ●) and different ratios of starting materials **3** and **4** (molar ratio: 1:1 ●/■; 10:1 ▲).

Under the assumption that the reaction of phosphane **3** with a 10-fold excess of azide **4** behaves like a pseudo first order reaction, the rate constant k_{obs} was calculated according to equation 1 [46].

$$\tau_{1/2} = \frac{ln2}{k'} \quad mit\ k' = k_{obs} \cdot [azide]$$

With a concentration of 710 nM of azide **4**, k_{obs} is calculated with a value of $0.7 \cdot 10^{-3}$ $M^{-1}s^{-1}$. This is in good agreement with other results found in the literature for the Staudinger ligation [34]. Although other bioorthogonal reactions proceed faster, the traceless Staudinger Ligation is suitable for radiolabeling purposes with fluorine-18 under mild reaction conditions.

Conclusion

Kinetic measurements of the reaction rate were accomplished to transfer and apply the traceless Staudinger Ligation for radiolabeling with short lived β^+ emitter fluorine-18. For this purpose, ^{19}F-NMR was used due to the presence of ^{19}F in the starting material (phosphane **3**) as well as in the corresponding product (amide **5**). The results of the measurements show a quite slow reaction rate, but clearly indicate that it is possible to apply the traceless Staudinger Ligation for ^{18}F-radiolabeling even in consideration of the short half-live of fluorine-18.

Experimental

Phosphanes **1**, **3**, **5** [28] and azide **4** [47] were synthesized as reported in the literature. NMR spectra of all compounds were recorded on an Agilent DD2-600 MHz NMR spectrometer (ProbeOne) at 25°C and chemical shifts of the ^{1}H, ^{13}C, and ^{31}P spectra were reported in parts per million (ppm) using TMS as internal standard for ^{1}H and ^{13}C, $CFCl_3$ for ^{19}F, and H_3PO_4 for ^{31}P spectra. Deuterated solvents were purchased from Deutero. For all kinetic NMR experiments, stock solutions of phosphane **3** were prepared with a concentration of 71 nM and azide **4** with final concentrations of 71 nM and 710 nM, respectively, using a mixture of acetonitrile-d_3 and D_2O (*v*:*v* = 10:1). 300 μL of each solution was combined into an NMR tube to reach a final solvent amount of 600 μL. At the beginning of the reaction, ^{19}F and ^{31}P NMR spectra were recorded all 3 to 15 minutes, latter all 30 to 60 minutes. 16 scans were recorded for the recording of the ^{19}F and ^{31}P spectra. Measurements were accomplished using the standard pulse sequence from VnmrJ 4.2 software (Agilent). Determined signals were integrated and the values were plotted vs. time. Logarithmic plotting was used to determine the reaction half-life $\tau_{1/2}$ and the rate constant k_{obs} of the reaction. All NMR experiments were performed in triplicate. Diffraction data was collected with a Bruker-Nonius-Apex-II-diffractometer using graphite-monochromated Mo-Kα radiation (λ = 0.71073 Å). All diffraction measurement was done at –150 °C. The unit cell dimensions was recorded and refined using the angular settings of 7238 (**1**), and 9338 (**3**) reflections and the structures was solved by direct methods and refined against F^2 on all data by full-matrix least-squares using the program suits from Sheldrick [42,43,44]. All non-hydrogen atoms were refined anisotropically; all hydrogen atoms were placed on geometrically calculated positions and refined using a riding model. CCDC 1482485 (**1**) and CCDC 1482528 (**3**) contain the supplementary crystallographic data for this paper. These data can be obtained free of charge from The Cambridge Crystallographic Data Centre via www.ccdc.cam.ac.uk/data_request/cif.

References

1 Z.-P. A. Wang, C.-L. Tiana, J.-S. Zheng, RSC Adv. 5 (2015) 107192–107199.
2 G.T. Hermanson, Bioconjugate Techniques, 2nd ed., Academic Press, London, 2008.
3 D. M. Patterson, L. A. Nazarova, J. A. Prescher, ACS Chem. Biol. 9 (2014), 592–605.
4 S. Bondalapati, M. Jbara, A. Brik, Nature Chem. 8 (2016) 407–418.
5 M. Köhn, R. Breinbauer, Angew. Chem. Int. Ed. 43 (2004) 3106–3116.
6 S. S. van Berkel, M. B. van Eldijk, J. C. M. van Hest, Angew. Chem. Int. Ed. 50 (2011) 8806–8827.
7 C. I. Schilling, N. Jung, M. Biskup, U. Schepers, S. Bräse, Chem. Soc. Rev. 40 (2011) 4840–4871.
8 B. L. Nilsson, L. L. Kiessling, R. T. Raines, Org. Lett. 2 (2000) 1939–1941.
9 E. Saxon, J. I. Armstrong, C. R. Bertozzi, Org. Lett. 2 (2000) 2141–2143.
10 M. B. Soellner, K. A. Dickson, B. L. Nilsson, R. T. Raines, J. Am. Chem. Soc. 125 (2003) 11790–11791.
11 C. Grandjean, A. Boutonnier, C. Guerreiro, J.-M. Fournier, L. A. Mulard, J. Org. Chem. 70 (2005) 7123–7132.
12 R. Kleineweischede, C. P. R. Hackenberger, Angew. Chem. Int. Ed. 47 (2008) 5984–5988.
13 S. Liu, K. J. Edgar, Biomacromolecules 16 (2015) 2556–2571.
14 A. Bianchi, B. Bernardi, J. Org. Chem. 71 (2006) 4565–4577.
15 F. Nisic, G. Speciale, A. Bernardi, Chem. Eur. J. 18 (2012) 6895–6906.
16 O. David, W. J. N. Meester, H. Bieräugel, H. E. Schoemaker, H. Hiemstra, J. H. van Maarseveen, Angew. Chem. Int. Ed. 42 (2003) 4373–4375.

17 G. Masson, T. den Hartog, H. E. Schoemaker, H. Hiemstra, J. H. van Maarseveen, Synlett (2006) 865–868.
18 R. Pötzsch, S. Fleischmann, C. Tock, H. Komber, B. I. Voit, Macromolecules 44 (2011) 3260–3269
19 M. Pretze, F. Wuest, T. Peppel, M. Köckerling, C. Mamat, Tetrahedron Lett. 51 (2010) 6410–6414.
20 M. Pretze, A. Flemming, M. Köckerling, C. Mamat, Z. Naturforsch. B 65b (2010) 1128–1138.
21 C. Mamat, M. Franke, T. Peppel, M. Köckerling, J. Steinbach, Tetrahedron 67 (2011) 4521–4529.
22 C. Mamat, M. Köckerling Synthesis 47 (2015) 387–394.
23 M.-L. Tsao, F. Tian, P. G. Schultz, ChemBioChem 6 (2005) 2147–2149.
24 J.-M. Heldt, O. Kerzendörfer, C. Mamat, F. Starke, H.-J. Pietzsch, J. Steinbach, Synlett (2013) 432–436.
25 R. Wodtke, J. König, A. Pigorsch, M. Köckerling, C. Mamat, Dyes Pigm. 113 (2015) 263–273.
26 S. Bräse, C. Gil, K. Knepper, V. Zimmermann, Angew. Chem. Int. Ed. 44 (2005) 5188–5240.
27 M. F. Debets, C. W. J. van der Doelen, F. P. J. T. Rutjes, F. L. van Delft, ChemBioChem 11 (2010) 1168–1184.
28 C. Mamat, A. Flemming, M. Köckerling, J. Steinbach, F. R. Wuest, Synthesis (2009) 3311–3321.
29 A. Tam, M. B. Soellner, R. T. Raines, J. Am. Chem. Soc. 129 (2007) 11421–11430.
30 M. Pretze, D. Pietzsch, C. Mamat, Molecules 18 (2013) 8618–8665.
31 S. Richter, F. Wuest, Molecules 19 (2014) 20536–20556.
32 G. B. Saha, Fundamentals of Nuclear Pharmacy, 6th ed., Springer, New York – Heidelberg, 2010.
33 M. B. Soellner, B. L. Nilsson, R. T. Raines, J. Am. Chem. Soc. 128 (2006) 8820–8828.
34 F. L. Lin, H. M. Hoyt, H. van Halbeek, R. G. Bergman C. R. Bertozzi, J. Am. Chem. Soc. 127 (2005) 2686–2695.
35 P. W. Miller, N. J. Long, R. Vilar, A. D. Gee, Angew. Chem. 2008, 120, 9136–9172.
36 W.R. Dolbier, Guide to Fluorine NMR for Organic Chemists. 1st Vol., 2009, John Wiley & Sons, Hoboken, New Jersey, USA.
37 D. L. Rabenstein, Anal. Chem. 73 (2001) 214A–223A.
38 R. Martino, V. Gilard, F. Desmoulin, M. Malet-Martino, J. Pharm. Biomed. Anal. 38 (2005) 871–891.
39 O. Herd, A. Heßler, M. Hingst, M. Tepper, O. Stelzer, J. Organomet. Chem. 522 (1996) 69–76.
40 O. Herd, A. Heßler, M. Hingst, P. Machnitzki, M. Tepper, O. Stelzer, Catal. Today 42 (1998) 413–420.
41 C. Mamat, A. Flemming, M. Köckerling, Z. Kristallogr. NCS 225 (2010) 345–346.
42 G. M. Sheldrick, SHELXS-97 and SHELXL-97, Programs for the Solution and Refinement of Crystal Structure; University of Göttingen: Göttingen, 1997.
43 G. M. Sheldrick, Acta Cryst. A 64 (2008) 112–122.
44 G. M. Sheldrick, Acta Cryst. C 71 (2015) 3–8.
45 E. V. Anslyn, D. A. Dougherty, Modern Physical Organic Chemistry. University Science Books, USA, 2005.
46 I.N. Levine, Physical Chemistry. 4th ed., McGraw-Hill, 1995, chapt. 17.
47 L. Campbell-Verduyn, P. H. Elsinga, L. Mirfeizi, R. A. Dierckx, B. L. Feringa, Org. Biomol. Chem. 6 (2008) 3461–3463.